

University of Groningen

Electron spin transport in graphene and carbon nanotubes

Tombros, Nikolaos

IMPORTANT NOTE: You are advised to consult the publisher's version (publisher's PDF) if you wish to cite from it. Please check the document version below.

Document Version

Publisher's PDF, also known as Version of record

Publication date:

2008

[Link to publication in University of Groningen/UMCG research database](#)

Citation for published version (APA):

Tombros, N. (2008). *Electron spin transport in graphene and carbon nanotubes*. s.n.

Copyright

Other than for strictly personal use, it is not permitted to download or to forward/distribute the text or part of it without the consent of the author(s) and/or copyright holder(s), unless the work is under an open content license (like Creative Commons).

Take-down policy

If you believe that this document breaches copyright please contact us providing details, and we will remove access to the work immediately and investigate your claim.

Downloaded from the University of Groningen/UMCG research database (Pure): <http://www.rug.nl/research/portal>. For technical reasons the number of authors shown on this cover page is limited to 10 maximum.

9

Electronic measurements on a single superconducting tin nanowire encapsulated in a multiwalled carbon nanotube¹

The charge transport properties of single superconducting tin nanowires, encapsulated by multiwalled carbon nanotubes have been investigated by multi-probe measurements. The multiwalled carbon nanotube protects the monocrystalline tin nanowire from oxidation and shape fragmentation and therefore allows to investigate the electronic properties of stable wires with diameters as small as 25 nm. The transparency of the contact between the Ti/Au electrode and nanowire can be tuned by argon ion etching the multiwalled nanotube. Application of large electrical current results in local heating at the contact which in turn suppresses superconductivity.

¹N. Tombros *et al*, submitted to Nano Letters

9.1 Introduction

Superconducting one-dimensional wires with diameters smaller than the phase coherence length, $\xi(T)$, show nonzero electrical resistance far below the superconducting transition temperature T_c . A possible origin of this remarkable effect are quantum phase slip processes [1]. However, experiments performed in granular [2], polycrystalline [3] and amorphous wires [4] give conflicting results, due to the different microstructure and morphology of the wires [5]. Performing experiments on a system having the least possible variations in morphology and microstructure could not only clarify the mechanisms of phase slip processes but also allow the exploration of new properties [6,7]. Promising candidates for such studies are single-crystalline Sn or Pb nanowires [8,9]. Up to now the majority of the electronic measurements have been performed on parallel arrays of nanowires embedded in a polycarbonate membrane and hence have the drawback that the measured resistance is a response from several or even thousands of parallel nanowires, which can be different in crystallinity and size. It is extremely difficult to fabricate an electronic device with a single monocrystalline Sn nanowire with the help of electron beam lithography, since the wires undergo strong oxidation when released from the porous membrane [9,10]. Furthermore, Sn wires with diameters smaller than 70 nm are very unstable at room temperature, resulting in fragmentation within a few hours during sample fabrication [9,11]. Therefore, electronic measurements on a single very thin ($\ll 70$ nm) Sn wire are extremely demanding or perhaps even impossible if one uses the systems described above. However, we succeeded in making electric contacts to Sn nanowires of diameters as small as 25 nm. Here, the Sn nanowire was completely surrounded by a multiwalled carbon nanotube [12] and therefore protected from oxidation and from shape fragmentation.

9.2 Experiment

Multiwalled carbon nanotubes encapsulating single-crystalline tin nanowires (Sn-CNT) [12] were dispersed in HPLC grade chlorobenzene and subjected to mild sonication (<40 Watt) for 1 min. A droplet of the suspension was deposited on a Si/SiO₂ substrate and dried with nitrogen. We used a scanning electron microscope (SEM) at 20 kV to locate the Sn-CNTs on the SiO₂ surface and measure their thickness. Inspection showed that the majority of the nanotubes was completely filled with Sn, had a length smaller than 1.5 μm and a diameter around 50 nm. SEM and transmission electron microscopy [12] evidenced that the carbon walls of the nanotube contribute about 10 nm to the total diameter. Therefore a 50 nm multiwalled nanotube contains a 40 nm diameter Sn nanowire.

The smallest Sn nanowire that we managed to contact with electrodes was 25 nm thick. Conventional electron beam lithography was used to pattern the electrodes on top of a single Sn-CNT. Prior to the evaporation of metals we applied argon ion etching (20 Watt power at 800 V acceleration for 15 to 75 seconds) to the places where the electric contacts were successively made. We avoided longer etching times because this can destroy the tin nanowire, as the etching speed of tin (26 nm/min) in our system is much larger than that of graphite (0.4 nm/min). This procedure partially removed the carbon walls, making it possible to place the metallic probes (Ti, Au) either in direct contact to the Sn wire or, if not all the carbon protection was removed at the contact point, in indirect contact through a tunnel barrier. With an electron bombardment evaporating system operating at $1.0 \cdot 10^{-6}$ mbar, a 1.2 nm thick layer of Ti was evaporated as an adhesion layer and 160 nm of Au were deposited on top by thermal sublimation (Fig. 9.1a). Electronic measurements on Sn-CNTs which were not subject to argon etching did not show any sign of superconductivity. In this case the Ti/Au electrodes make contact to the carbon walls of the multiwalled nanotube through contact resistances of several $M\Omega$'s.

We preferred an etching procedure which did not completely remove all carbon layers to ensure a minimum diffusion [13] of Ti and Au into the Sn nanowire, as the remaining carbon atoms between the Ti-Au and the Sn wire act as a natural diffusion barrier (Fig. 9.1b) [13]. We succeeded in making 5 devices on Sn nanowires, having at least 4 probes with contact resistances low enough to measure the resistivity at temperatures between room temperature and 1.5 K. A qualitative agreement was found between increasing etching times and the decrease in contact resistance, however, full control of this process was not achieved. The resistance was measured using the standard ac lock-in technique, with frequencies in the range 7 Hz to 340 Hz and currents $I_{ac} < 20$ nA. The diameter of each individual wire in each of the 5 devices was constant along its length, the thinnest measuring 25 nm and the thickest 40 nm. The resistivity of the wires ranged between 12.5 to 16 $\mu\Omega$ cm at room temperature (RT) and 1.4 to 3.4 $\mu\Omega$ cm at 4.2 K. Dividing the value of the resistivity at RT by the one at 4.2 K gives a residual resistance ratio $RRR = R_{RT}/R_{4.2K}$ between 5 and 10, which is similar to the values found in other studies on Sn nanowires [9]. Furthermore, using the free electron model, we found an elastic mean free path for the electrons in the range 15 to 35 nm, never exceeding the diameter of the wire. This low value can be the result of enhanced surface scattering in the system. The highest value of $T_c = 3.6$ K is measured for a device in which a 31 ± 2 nm wire is contacted by Ti/Au electrodes separated by $\Delta L = 400$ nm. This is slightly lower than the T_c of bulk tin (3.72 K). The lowest T_c of 3 K was measured for samples having contact resistances lower than 150Ω and spacing between the electrodes of $\Delta L = 240$ nm. A typical

four probe resistance of a 40 ± 2 nm diameter nanowire is depicted in Fig. 9.1c (contact resistances ~ 1 k Ω , $\Delta L = 240$ nm). Striking is not only the T_c of 3.2 K but also the nonzero value of the resistance at $T = 1.7$ K. Quantum phase slip is expected to result in a finite resistance at $T \ll T_c$. However, in our system, in which the superconductor is contacted to normal metals, we believe that proximity effect is the main mechanism. Boogaard *et al.* [14] showed that the proximity effect not only results in a finite resistance of the superconductor, but also in a decrease in T_c . Applying an external magnetic field B , enabled us to suppress superconductivity (insert Fig.9.1c). The critical field was about 600 mT at $T = 1.5$ K for a 40 ± 2 nm diameter Sn wire. Using the relation $H_c(T) = H_c(0)(1-(T/T_c)^2)$ we obtained a remarkably high critical field $H_c(0) = 800$ mT. Such a huge critical field is expected for nanowires having a mean free path, l , smaller than the coherence length ξ_0 (dirty limit) [6]. In this case the critical field B_{dl} has a value close to $B_{cl}\sqrt{\xi_0/l}$, with B_{cl} the critical field for a superconductor in the clean limit ($B_{cl} = 0.908 \mu_0\Phi_0/\xi_0d$, with d the diameter of the wire and $\Phi_0 = h/2e$ the flux quantum). For $d = 40$ nm we expect $B_{cl} = 220$ mT. Taking into account that $l = 20$ nm for the 40 nm diameter wire and $\xi_0 \sim 230$ nm, we obtain a value of 750 mT for B_{dl} , a value close to the experimental one. Obviously thinner nanowires in the dirty limit can have even larger critical magnetic fields.

In most studies, the superconducting wires were contacted by only two probes [2–4,9,10,15]. In our samples we were able to perform 3 probe measurements. This made it possible to investigate the effect of each individual contact resistance on the Sn wire. Fig. 9.2a presents the normalized differential resistance ($dV/dI/R_n$) of different contacts on three Sn wires. The contact between the Ti-Au electrode and the tin nanowire can be a tunnel barrier or a clean contact. The different families of differential conductance traces found between the two extremes (clean contact vs tunnel barrier) for a superconductor-normal metal junction, have been investigated by Blonder, Tinkham and Klapwijk (BTK) [16, 17]. In the BTK model the strength of the barrier is given by the dimensionless parameter Z . For a clean contact $Z = 0$ and for a tunnel junction $Z \gg 1$. In our system a tunnel junction could be formed when the interface between the electrode and the tin consists of a single or several carbon nanotube walls and/or a thin Ti-carbide layer. In Fig. 9.2a, the contact with highest resistance also gave the highest Z value with $Z = 1.2$, showing tunneling type behavior. In general, high contact resistances showed a monotonic increase in the zero bias resistance when the temperature became smaller than T_c . (curves a1, a2 and c1 Fig. 9.2a Reflection at the interface between the normal metal (Au) and the superconductor (Sn wire) is responsible for this behavior. On the other hand, a decrease in the resistance was found when the contact resistances were low, usually below 2k Ω . (curves b1, c2, a3) Here, Andreev reflection takes place at the interface and in the ultimate

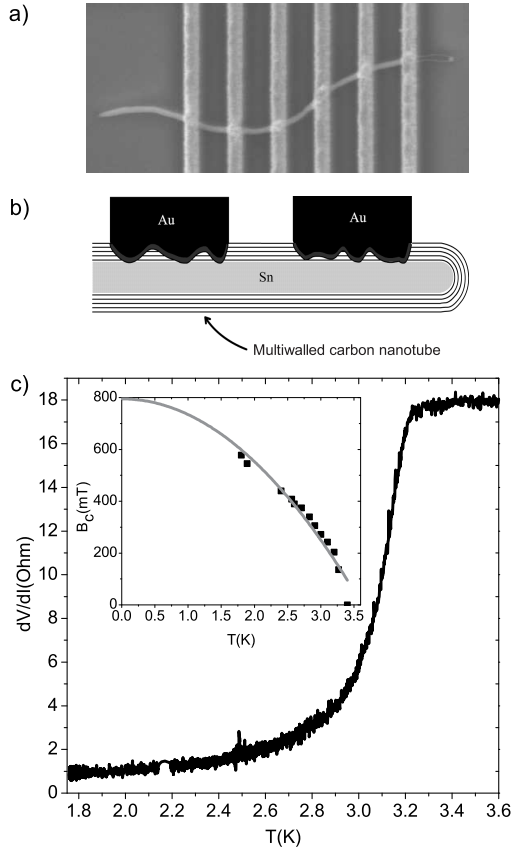


Figure 9.1: a) Image of a typical tin carbon nanotube (Sn-CNT) device taken with a scanning electron microscope. The Sn-CNT has a diameter of $d = 50 \pm 2$ nm (Sn nanowire $d = 40 \pm 2$ nm) and is lying on a SiO_2 surface. The electrodes are composed of a 1.2 nm Ti adhesion layer and 160 nm of Au. The distance between electrodes is $\Delta L = 250$ nm. b) A cartoon showing the contact between the Ti/Au contacts and the Sn. Electronic measurements suggest small contact areas. c) A typical four probe measurement, of the resistance of the Sn wire ($\text{RRR} = 5.5$) as function of temperature. Superconductivity sets in at 3.2 K, far below the T_c of bulk tin (3.72 K). The resistance remains non-zero at temperatures $\ll T_c$. Inset shows the critical field at which superconductivity is completely suppressed. The data are fitted giving $T_c = 3.55$ K and a remarkably high critical field of 800mT.

case, namely the clean interface ($Z=0$), this should result in a resistance (at $T \ll T_c$) equal to the half of the resistance just above T_c . Remarkably, the superconducting transition temperature of the thinnest nanowire ($T_c = 3.6$ K, $d = 31 \pm 2$ nm) in Fig. 9.2a (curves c1 and c2) was much higher than that of the other two wires. This enhancement can not be explained by the proximity effect. All the three wires had contact resistances in the same range and equal spacings between the electrodes and hence the influence of the proximity effect on the critical temperature should be the same for all. An enhancement in T_c was also observed in experiments performed on parallel arrays of Sn nanowires embedded in a polycarbonate membrane [9]. There, Tian *et al* found an increase by 0.4 K in the T_c of 20 nm diameter Sn nanowires with respect to the T_c of wires with $d > 40$ nm. A shape-dependent superconducting resonance effect could be the origin of this enhancement [18].

We suppressed superconductivity in the system by applying an external magnetic field oriented parallel to the long axis of the Sn wire as clearly visible in the contact resistance reported in Fig. 9.2b. The critical field was about 270 mT for the 49 ± 2 nm diameter Sn wire ($l = 30$ nm). This corresponds to a $B_c(0) = 340$ mT and is almost 40 % lower than the value expected for the dirty limit ($B_{dl} = 540$ mT). In general, for nanowires with the same diameter we observed a broad range of critical fields (both for 2 probe and 4 probe measurements). For example, for 35 nm Sn wires (4 samples) we found critical fields in the range 450 to 600 mT at $T = 1.5$ K.

For a 50 nm diameter Sn wire we expect a critical current density of $J_c = 10^7$ - 10^8 A/cm² [1] hence applying a dc current with density J_c should suppress superconductivity [19]. However, Fig. 9.3a shows this effect at a current of $I_p = 1.25$ μ A corresponding to a density of 10^5 A/cm², i.e. 2 to 3 orders of magnitude smaller than J_c . Close examination of the contact resistances reveals (Fig. 9.3a) that the suppression of superconductivity happens very locally at the contact region and not in the Sn wire itself. Possible causes can be local heating or reaching the critical current at a pinhole at the contact. The latter is, however, unlikely since the current would have to generate a magnetic field equal to the critical magnetic field over a distance $\lambda(T)$, which clearly does not occur. A simple model allows us to find the relation between I_p and the local heating at a contact with resistance R_n : a current I_p generates a power $P = I_p^2 R_n = -SK(T)dT/dx$, at the contact; the heat flux moves away from the contact through the gold electrode with cross section area $S \sim 0.04$ μ m² and thermal conductivity $K(T) = K_c T$. Solving the above equation using the boundary conditions $T = T_c$ at $x = 0$ and $T = T_0$ at $x \sim 1$ μ m gives $I_p \sim (1/\sqrt{R_n})\sqrt{1 - (T_0/T_c)^2}$. Both, the $1/\sqrt{R_n}$ dependence of I_p at $T=1.5$ K (Fig. 9.3b, 8 different samples with contact resistances in the range $R_0 = 6$ Ω - 40 k Ω) and the temperature dependence of I_p

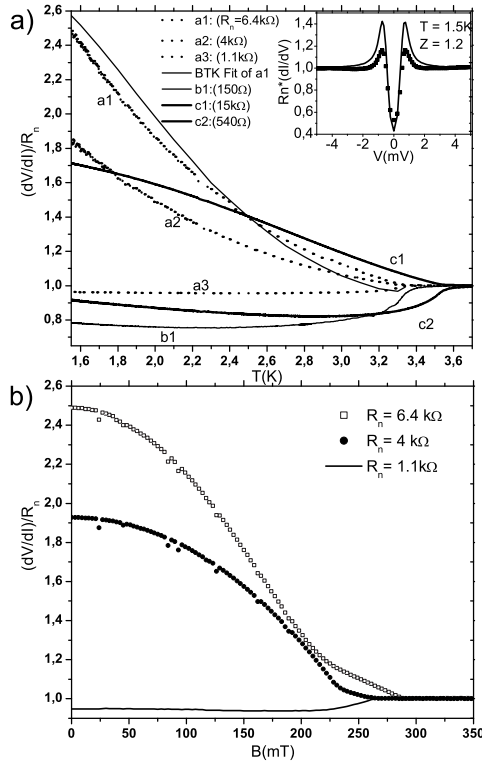


Figure 9.2: Contact resistances between a Ti/Au electrode and a Sn nanowire a) Curves a1, a2 and a3 correspond to a Sn wire with $d = 49 \pm 2$ nm, curve b1 to one with $d = 46 \pm 2$ nm, and c1 and c2 to a wire with $d = 31 \pm 2$ nm wire. The differential contact resistance are normalized to the value of the contact resistance R_n at $T = 4.2$ K. For the nanowire with diameter $d = 49 \pm 2$ nm the contact with highest resistance ($R_n = 6.4$ k Ω) is fitted by the BTK model giving a barrier $Z = 1.2$. The inset shows the normalized differential conductance of this contact together with the BTK fit. The peak position at ± 0.7 mV corresponds to the superconducting gap at $T = 1.5$ K b) $T = 1.5$ K. Application of an external magnetic field aligned along the axis of the homogeneous nanowire gives similar critical fields (~ 270 mT) for all three contacts characterized by the curves a1, a2 and a3 in panel a).

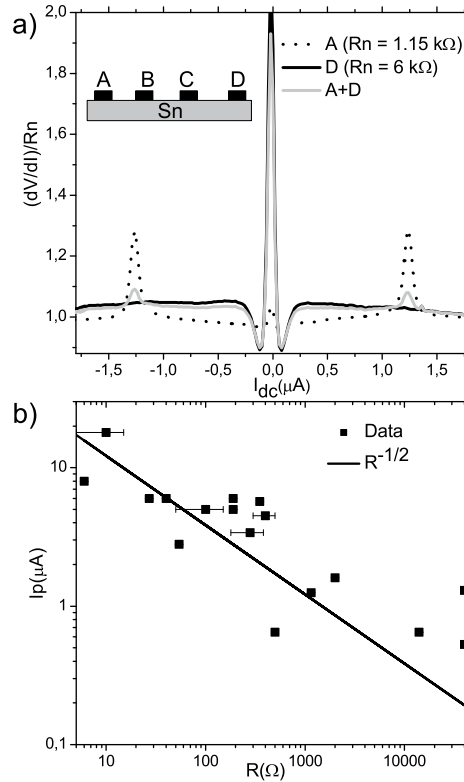


Figure 9.3: a) The inset schematically shows a encapsulated Sn wire contacted by 4 Ti/Au electrodes. A two probe measurement (curve A + D) shows a peak at $I_{dc} = \pm 1.25 \mu\text{A}$ however, it does not provide enough information about its origin. The presence of the peak in the normalized differential resistance of contact A and its absence in contact D suggests local heating or a critical current reached at a pinhole at contact A as its origin. b) Peak position I_p as a function of contact resistance R_n in a log-log plot ($T = 1.5 \text{ K}$, 8 samples). A $1/\sqrt{R_n}$ dependence is expected for local heating.

(Fig. 9.4) support that idea that heating causes the suppression of superconductivity in this temperature range. However, the deviation from the heating model found at low temperatures in Fig. 9.4b suggests that other processes become more important. One of the processes is the creation of phase slip centers inside the nanowire [10]. The most interesting processes, the quantum phase slip pro-

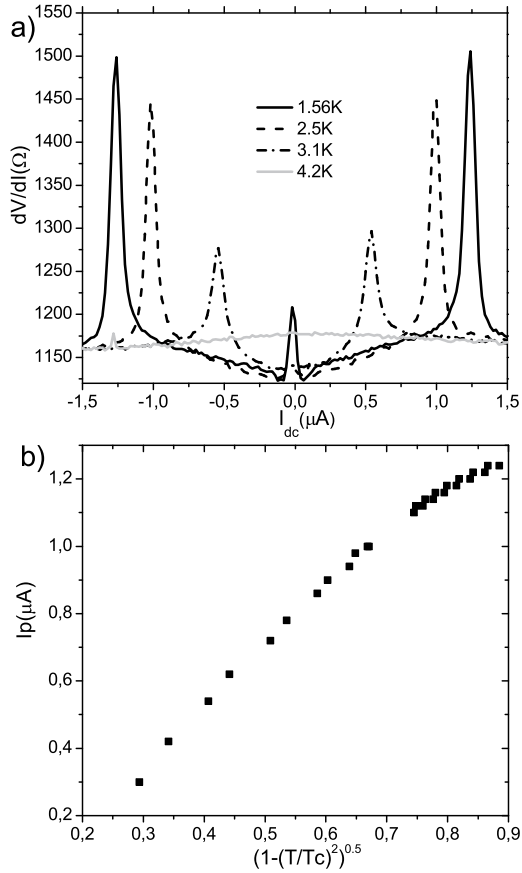


Figure 9.4: a) Differential resistance of contact *A* (Fig. 9.3) as a function of the dc bias for several temperatures. The peak is at position I_p (at $\pm 1.25 \mu A$ for $T = 1.56 K$) which decreases as a function of temperature. b) Heating at the contact should give a $\sqrt{1 - (T/T_c)^2}$ ($T_c = 3.4 K$) dependence for I_p . We observe a linear dependence for temperatures higher than 2.5 K indicating that heating affects the peak position in this temperature range. The deviation found at lower temperatures shows that other processes become important too.

cesses are expected to dominate in very thin nanowires ($\ll 25 nm$). Those new type of ultrathin monocrystalline nanowires could become available for electronic measurements if they are protected from oxidation and shape fragmentation. A

promising candidate in this direction is a tin nanowire encapsulated in a multiwall carbon nanotube or in the ultimate limit, in a single wall carbon nanotube.

9.3 Conclusions

Summarizing, we have succeeded in making electric contacts to Sn nanowires of diameters as small as 25 nm. The wires are encapsulated in a multiwalled carbon nanotube and thus protected from oxidation and shape fragmentation. The critical temperature for superconductivity in wires with diameters between 25 and 40 nm was found to range from 3 to 3.6 K, due to the proximity effect ensuing from the metal-superconductor interface. The critical magnetic field in this type of wires was determined to be as high as 800 mT. As a next step we intend to contact even thinner nanowires with superconducting contacts to allow the investigation of quantum phase slip processes. Our system opens new possibilities to the investigation of superconducting properties of ultrathin nanowires and could become a model system in nanoscience. A fascinating application of superconducting nanowires may be in quantum optics, where these wires can be used as single photon detectors, tuning in to quantum encrypted information [20].